

# Phase Transition Characteristics of Flame-Synthesized Gamma- $\text{Al}_2\text{O}_3$ Nanoparticles with Heat Treatment

Gyo Woo Lee

**Abstract**—In this study, the phase transition characteristics of flame-synthesized  $\gamma\text{-Al}_2\text{O}_3$  nanoparticles to  $\alpha\text{-Al}_2\text{O}_3$  have been investigated. The nanoparticles were synthesized by using a coflow hydrogen diffusion flame. The phase transition and particle characteristics of the  $\text{Al}_2\text{O}_3$  nanoparticles were determined by examining the crystalline structure and the shape of the collected nanoparticles before and after the heat treatment. The morphology and crystal structure of the  $\text{Al}_2\text{O}_3$  nanoparticles were determined from SEM images and XRD analyses, respectively. The measured specific surface area and averaged particle size were  $63.44\text{m}^2/\text{g}$  and  $23.94\text{nm}$ , respectively. Based on the scanning electron microscope images and x-ray diffraction patterns, it is believed that the onset temperature of the phase transition to  $\alpha\text{-Al}_2\text{O}_3$  was existed near  $1200^\circ\text{C}$ . The averaged diameters of the sintered particles heat treated at  $1,260^\circ\text{C}$  were approximately  $80\text{nm}$ .

**Keywords**—BET Specific Surface Area, Gamma- $\text{Al}_2\text{O}_3$  Nanoparticles, Flame Synthesis, Phase Transition, X-ray Diffraction.

## I. INTRODUCTION

ALUMINA is one of the most widely used ceramic materials as catalysts, catalyst supports and absorbents, and also wear resistant coating [1], [2]. Alumina is an electrical insulator but has a relatively high conductivity for a ceramic material. Being chemically inert and white, alumina is favored filler for plastics. Also, it is a common ingredient in sunscreen and lots of cosmetics. Alumina is a catalyst itself for converting hydrogen sulfide waste gases into elemental sulfur. Also, alumina is used as a catalyst support for many industrial applications. The most common occurring crystalline form, alpha-alumina, makes it suitable for use as an abrasive and as a component in cutting tools. The other phases, gamma-, delta-, eta-, theta-, and chi-alumina are also existed.

There are lots of production method for alumina powders like sol-gel process [3]-[6], hydrothermal method [7], co-precipitation process, mechanical milling, vapor phase reaction, and combustion method [8], [9]. As the process temperature goes higher the more phase transition to gamma-, delta-, theta-, and alpha-alumina can be occurred. These transitions were accompanied with abrupt decrease in specific surface area thru the sintering process among particles, especially from gamma to alpha phase. Most of the production methods tend to be multi-phased, and should be optimized for

tailored production. Used as a structural material alpha alumina with high strength is needed. Also, the gamma alumina with large specific surface area is suitable for the heat-resisting catalyst support. It is not easy to get nano-sized alpha alumina thru the calcination process which accompanied with grain growth of the nano particles.

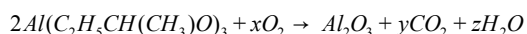
Park and Jung [1] reviewed the flame synthesis and flame spray pyrolysis for the production of gamma alumina, and also introduced an aerosol process for the alpha alumina synthesis. Mirjalili et al. [2] reported the effect of stirring time on the synthesis of nano scaled alpha alumina particles. Alumina nanoparticles were synthesized through alkoxide route using sol-gel method. Calcination process was ranged from  $1,000^\circ\text{C}$  to  $1,200^\circ\text{C}$ . Jiang et al. [3] and Ming et al. [4] also showed the production process for alpha and gamma alumina, respectively. Spherical porous alumina particles were prepared by mixed solvent to control the reaction rate of Al-alkoxide and the particle shape with hydroxyl-propyl cellulose [5]. As the  $\text{H}_2\text{O}/\text{Al-alkoxide}$  ratio increase, the crystal structure of as-prepared particles was continuously varied from amorphous  $\text{Al}(\text{OH})_3$  to pseudo-boehmite with chemical composition of  $\text{AlO}(\text{OH})$ . In 2005, Lee et al. [6] fabricated the composite alumina by adding various promoters by sol-gel method and examined their thermal stability. They reported the similar delay of phase transition by adding silica and lanthanum. Prior to this, Youn et al. [7] showed that the addition of alumina-sol into gamma alumina enabled the onset of the gamma to alpha transformation at temperature as low as  $600^\circ\text{C}$ . Park et al. [8] prepared aluminum oxide particles by the hydrolysis of aluminum oxide alkoxides followed by calcinations, in the presence of surface stabilizing agents, such as  $\text{Na}(\text{AOT})$  ( $\text{C}_{20}\text{H}_{37}\text{NaO}_7$ , sodium bis-2-ethylhexyl sulfosuccinate) molecules. They investigated several parameters to control the particle size. An analysis of the morphology and crystal structure of commercial gamma alumina nanoparticle was presented by Rozita et al. [9] in 2009. Characterization was carried out with a combination of several techniques such as transmission electron microscope (TEM), scanning electron microscope (SEM), energy dispersive x-ray analysis (EDX), selected area electron diffraction (SAED), and x-ray diffraction (XRD).

Due to the relative easiness of doping and scale-up than the other method, the production of alumina by using a flame is focused by lots of researchers. Johannessen et al. [10] presented a mathematical model for the dynamics of particle growth during synthesis of ultrafine particles in diffusion flames. The

G. W. Lee, Associate Professor, is with the Division of Mechanical Design Engineering, Chonbuk National University, in Jeonju, Jeonbuk 561-756, South Korea (e-mail: gwlee@jbnu.ac.kr).

model included the kinetics of particle coalescence and coagulation, and when combined with a calculation of the temperature, velocity and gas composition distribution in the flame, the effluent aerosol characteristics were calculated. The estimated kinetics can be used to predict the surface area and shape of the particles for a wide range of synthesis conditions. In 2006, Kelekanjeri et al. [11] synthesized alpha alumina thin film on fused silica and nichrome substrates using a combustion chemical vapor deposition process.

Aluminum Tri-Sec-Butoxide (ATSB,  $\text{Al}[\text{C}_2\text{H}_5\text{CH}(\text{CH}_3)\text{O}]_3$ ) is used as a precursor for the alumina nanoparticles in this study, and the overall oxidation reaction is as below [10].



In this study, the phase transition characteristics of flame-synthesized  $\gamma\text{-Al}_2\text{O}_3$  nanoparticles to  $\alpha$ -phased ones have been investigated. The nanoparticles were synthesized by using a coflow hydrogen diffusion flame. The morphology, specific surface area, and crystalline phase of the synthesized  $\text{Al}_2\text{O}_3$  nanoparticles before and after the heat treatment were analyzed by electron microscope, particle size analyzer, and x-ray diffractometer, respectively. The collected nanoparticles were heat treated at 200, 900, 1100, 1180 and 1260 °C to compare the thermal stability of alumina nanoparticles.

## II. EXPERIMENTAL

The experimental set-up for flame synthesis consisted of several gases and mass flow controllers with readout units (Kofloc Co. Ltd, Kyoto, Japan), a temperature controlled evaporator for the precursor, a burner and a flame that were used as a reactor, a two dimensional traversal system for moving the burner and a one-dimensional traversal system with a controller for particle sampling. The diffusion flame burner used in this study had three concentric tubes of inner diameters of 3.87, 16.57 and 70.0 mm. Aluminum Tri-Sec-Butoxide (ATSB,  $\text{Al}[\text{C}_2\text{H}_5\text{CH}(\text{CH}_3)\text{O}]_3$ ; Sigma Aldrich Korea Co.; purity .97%) was used as the precursor for alumina nanoparticles. The precursor was used without any further purification. The argon that was used as the carrier gas for the precursor was delivered through a central tube via the evaporator of ATSB. The evaporator was maintained at temperature of 170°C. The fuel, namely, hydrogen, was supplied through the second tube. The air was passed through the outer tube, which was the third tube. The experimental conditions regarding the flowrates of the gases are provided in Table I.

TABLE I  
EXPERIMENTAL CONDITIONS

Gas	Ar	H <sub>2</sub>	O <sub>2</sub>	N <sub>2</sub>	Air	O <sub>2</sub> Concentration of Oxidizer	Precursor (ATSB) Evaporation Temperature
Function	ATSB	Fuel	Oxidizer				
Flow Rates (liters/min.)	0.3	2.0	0.0	0.0	33.7	21 %	170 °C
Tube Inner Diameter (mm)	3.87	16.57	70.0			-	-

The synthesized nanoparticles were collected on a thermophoretic plate that was placed at 230mm height above the burner. Then, the collected nanoparticles were heat treated at several temperatures, namely, 200, 900, 1100, 1180 and 1260 °C, for two hours. The temperature of 200 °C was selected for drying the formed nanoparticles. A field emission scanning electron microscope (FE-SEM S-4700, Hitachi Inc. Japan, in KBSI Jeonju Center), X-ray diffraction (XRD, DMAX-2500, Rigaku Inc., Tokyo, Japan) and specific surface area (UPA-150, Microtrac, USA) analyses were used for the characterization of the nanoparticles before and after heat treatment. A schematic diagram of the experimental procedure is shown in Fig. 1.

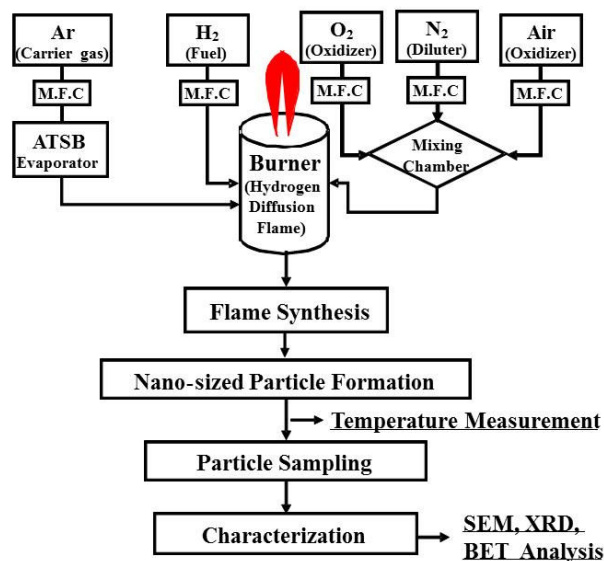


Fig. 1 Experimental procedure

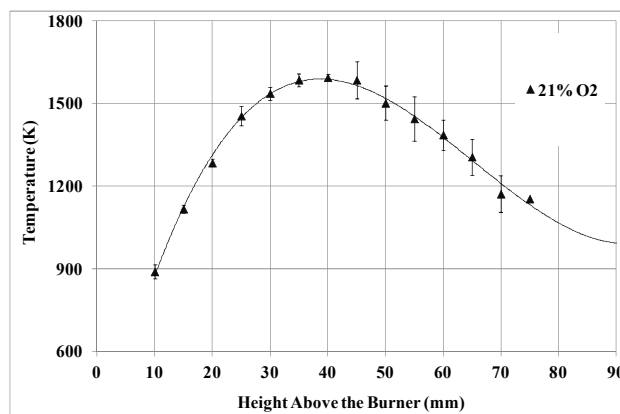


Fig. 2 Averaged axial temperatures and standard deviations with height above the burner

### III. RESULTS AND DISCUSSION

#### A. Axial Temperature Distribution of the Flame

Using fine-wired ( $50\mu$  m in diameter) R-type thermocouples (Pt / Pt-13%Rh, SP13RH-002, Omega Engineering Inc.), the axial temperature distributions of the several flames were measured and shown in Fig. 2. Through our previous results [12] we knew that the use of air as an oxidizer in the diffusion flame burner was good enough to produce the smaller particles with the larger specific surface area than the other flames using oxygen enriched air. The maximum centerline temperature was measured to be 1,594K at 40mm height above the burner. The measured specific surface area and calculated particle diameter was  $63.44\text{m}^2/\text{g}$  and  $23.94\text{nm}$ , respectively [12]. In Fig. 2, the temperature measurement was done without feeding the ATSB (only argon gas was supplied thru the center tube) in the flame. The radiation heat loss of the thermocouple junction was compensated.

The temperature distribution was lower than expectation. Through this distribution the representing value of flame synthesis and the location of thermophoretic collection were determined.

#### B. Particles Characteristics thru SEM Analysis

To know the particle characteristics like particle size and shape scanning electron microscope images were investigated. Fig. 3 shows the alumina nanoparticles heat-treated for two hours at  $200^\circ\text{C}$  (a),  $900^\circ\text{C}$  (b),  $1,100^\circ\text{C}$  (c),  $1,180^\circ\text{C}$  (d), and  $1,260^\circ\text{C}$  (e). Since the phase transition of alumina is ranged from  $1,100^\circ\text{C}$  to  $1,200^\circ\text{C}$  in general, the heat treatment temperatures were chosen near  $1,100^\circ\text{C}$ , and  $200^\circ\text{C}$  was selected for drying the collected powders.

In the images, there's no significant change in shape and size of the particles when the heat treatment temperature was lower than  $1,100^\circ\text{C}$ . In case of particles heat-treated at  $1,180^\circ\text{C}$ , Fig. 3 (d), some particles were sintered with each other and larger particles were formed. When the heat treatment was done at  $1,260^\circ\text{C}$ , Fig. 3 (e), all the particles were sintered and formed much larger particles. Before the sintering, Figs. 3 (a), (b), and (c), particle diameters were approximately ranged from 20 to 25 nm. But after the sintering, Fig. 3 (e), particles looks larger than 100 nm in diameter.

#### C. BET Specific Surface Area

To quantify the qualitative microscope image analysis, the BET (Brunauer–Emmett–Teller) specific surface areas were measured. Fig. 4 shows these measured surface areas and particle diameters with heat treatment temperatures. The particle diameters were calculated from the measured specific surface areas and well-known density of alumina,  $3.95\text{g}/\text{m}^3$ .

When heat-treated at  $200^\circ\text{C}$  and  $900^\circ\text{C}$ , the specific surface areas of the particles were  $63.44\text{m}^2/\text{g}$  and  $63.38\text{m}^2/\text{g}$ , respectively. The particle diameter was approximately  $24\text{nm}$ . Above the temperature of  $1,100^\circ\text{C}$ , the higher heat treatment temperature the lower specific surface area. In cases of heat-treated at  $1,180^\circ\text{C}$  and  $1,260^\circ\text{C}$ , the specific surface areas

of the particles were  $55.72\text{m}^2/\text{g}$  and  $19.24\text{m}^2/\text{g}$ , respectively. Lots of sintered particles in Fig. 3 (e) were having a calculated diameter of  $78.94\text{nm}$ .

On the basis of the microscope images in Fig. 3 and the specific surface areas in Fig. 4, we believe that the sintering process of this experiment occurred at the heat treatment temperature of approximately  $1,200^\circ\text{C}$ .

#### D. X-Ray Diffraction Patterns

As told in the Introduction, alumina particles have several crystalline phases. To investigate the crystalline phase of the five heat-treated flame-synthesized alumina nanoparticles, x-ray diffraction analysis was done and shown in Fig. 5. From the previous results [12], originally formed nanoparticles were mainly gamma-phased and included partly theta-phased alumina. Gamma-phased alumina shows the three dominant peaks of diffraction intensity at  $2\theta=67, 46$ , and  $85^\circ$ . Similar with the SEM images in Fig. 3, the patterns in Fig. 5 shows that the particles heat-treated lower than  $1,100^\circ\text{C}$  remain gamma-phased. But the case of particles heat-treated at  $1,180^\circ\text{C}$ , the pattern shows the initiation of phase transition. It is well known that the dominant peaks for alpha phased alumina are existed at  $2\theta=43, 57, 32, 26$ , and  $68^\circ$ . Furthermore, in case of heat-treated at  $1,260^\circ\text{C}$  all the particles were transformed to alpha phase.

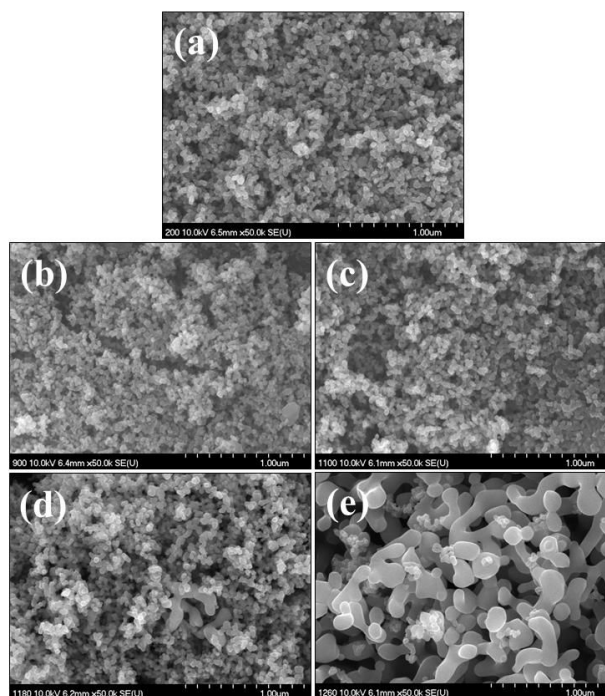


Fig. 3 SEM images of alumina nanoparticles after the two-hour heat treatment at (a)  $200^\circ\text{C}$ , (b)  $900^\circ\text{C}$ , (c)  $1100^\circ\text{C}$ , (d)  $1180^\circ\text{C}$ , and (e)  $1260^\circ\text{C}$

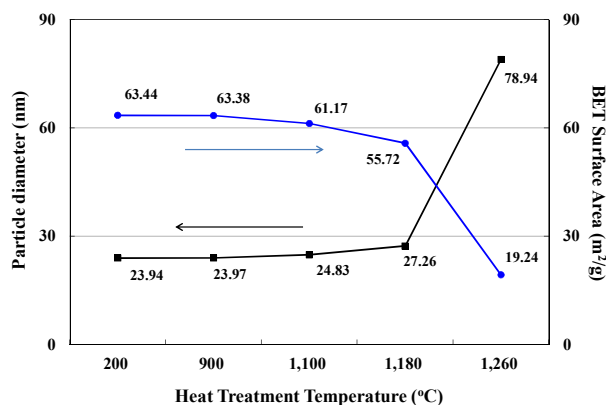


Fig. 4 Measured BET specific surface areas and calculated particle diameters of the heat-treated alumina nanoparticles

#### IV. CONCLUSION

In this work, the phase transition characteristics of flame-synthesized  $\gamma$ - $\text{Al}_2\text{O}_3$  nanoparticles to  $\alpha$ - $\text{Al}_2\text{O}_3$  have been studied. The measured specific surface area and averaged diameter of the synthesized alumina nanoparticles were 63.44  $\text{m}^2/\text{g}$  and 23.94 nm, respectively. Based on the electron microscope and x-ray diffraction analyses, it is believed that the onset temperature of the phase transition to  $\alpha$ - $\text{Al}_2\text{O}_3$  of this study was existed near 1200°C. The averaged diameters of the sintered particles heat treated at 1260°C were approximately 80 nm.

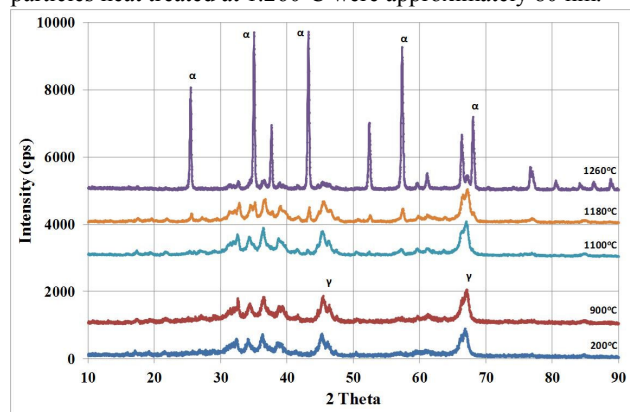


Fig. 5 X-ray diffraction patterns of the heat-treated alumina nanoparticles

#### ACKNOWLEDGMENT

This research was supported by Basic Science Research Program through the National Research Foundation of Korea (NRF) funded by the Ministry of Education, Science and Technology (2012-0002661).

#### REFERENCES

- [1] K. Y. Park, and K. Y. Jung, "Synthesis of nano-structured alumina powders thru the aerosol process," *Ceramist*, Vol. 12, No. 2, pp. 27-37, 2009.
- [2] F. Mirjalili, L. C. Abdullah, H. Mohamad, A. Fakhru'l-Razi, A. B. D. Radiah, and R. Aghabazadeh, "Process for producing

nano-alpha-alumina powder," *ISRN Nanotechnology*, Vol. 2011, Article ID 692594, pp. 1-5, 2011.

- [3] J. Li, Y. Pan, C. Xiang, Q. Ge, and J. Guo, "Low temperature synthesis of ultrafine  $\alpha$ - $\text{Al}_2\text{O}_3$  powder by a simple aqueous sol-gel process," *Ceramics International*, Vol. 32, No. 5, pp. 587-591, 2005.
- [4] M.-G. Ma, Y.-J. Zhu, and Z.-L. Xu, "A new route to synthesis of  $\gamma$ -alumina nanorods," *Mat. Lett.*, Vol. 61, No. 8-9, pp. 1812-1815, 2007.
- [5] U.-Y. Hwang, S.-W. Lee, J.-W. Lee, H.-S. Park, K.-K. Koo, S.-J. Yoo, H.-S. Yoon, and Y.-R. Kim, "Synthesis of porous  $\text{Al}_2\text{O}_3$  particles by sol-gel method," *J. of the Korean Inst. of Chemical Eng.*, Vol. 39, No. 2, pp. 206-212, 2001.
- [6] J.-W. Lee, H.-S. Yoon, U.-S. Chae, H.-J. Park, U.-Y. Hwang, H.-S. Park, D.-R. Park, and S.-J. Yoo, "A comparison of structural characterization of composite alumina powder prepared by sol-gel method according to the promoters," *Korean Chem. Eng. Res.*, Vol. 43, No. 4, pp. 503-510, 2005.
- [7] H.-J. Youn, J. W. Jang, I.-T. Kim, and K. S. Hong, "Low-temperature formation of  $\alpha$ -alumina by doping of an alumina-sol," *J. of Colloid and Interface Sci.*, Vol. 211, pp. 110-113, 1999.
- [8] Y. K. Park, E. H. Tadd, M. Zubris, and R. Tannenbaum, "Size-controlled synthesis of alumina nanoparticles from aluminum alkoxides," *Materials Res. Bulletin*, Vol. 40, pp. 1506-1512, 2005.
- [9] Y. Rozita, R. Brydson, and A. J. Scott, "An investigation of commercial gamma- $\text{Al}_2\text{O}_3$  nanoparticles," *J. of Physics: Conf. Series Vol. 241*, Article ID 012096, 2009.
- [10] T. Johannessen, S. E. Pratsinis, and H. Livbjerg, "Computational fluid-particle dynamics for the flame synthesis of alumina particles," *Chem. Eng. Sci.*, Vol. 55, pp. 177-191, 2000.
- [11] V. S. K. G. Kelekanjeri, W. B. Carter, and J. M. Hampikian, "Deposition of  $\alpha$ -alumina via combustion chemical vapor deposition," *Thin Solid Films*, Vol. 515, pp. 1905-1911, 2006.
- [12] G. W. Lee, "Particle Characteristics of Flame-Synthesized  $\gamma$ - $\text{Al}_2\text{O}_3$  Nanoparticles," *Trans. of the KSME(B)*, Vol. 36, No. 5, pp. 509-515, 2012.